NANOWIRE USED IN NANOTYPE GENERATORS FOR ENERGY HARVESTING

Aurelian COSTEA[1], Paul ŞCHIOPU[1,2], Marian VLĂDESCU[1,2]

Hitherto, to a large extent, the seebeck effect is used to build devices, nanogenerators, for thermoelectric energy harvesting. The difference in temperature between the nanogenerator two contact areas is the main factor relying on that drives the charge carriers spreading. Conventionally, thermoelectric devices have to have a gradient in temperature as a functional condition [1].We present a solution of thermal energy transformed to electric energy through pyroelectric properties of zincoxide nanorod matrices. Simultaneously harnessing the piezoelectric, semiconducting, also the pyroelectric characteristics of zincoxide, a polarization electric field was achieved [2]. Also, we noticed a electric charge segregation throughout the zincoxide caused by the time-conditioned temperature fluctuation.

Keywords: zincoxide nanowires, pyroelectric effect, nanogenerators, Schottky contact, Seebeck effect, piezoelectric effect

1. Introduction

Nanowires having piezoelectric properties made out of zincoxide are used for mechanical energy small-scale harvest. These nanogenerators are meant to take advantage of the piezopotential within the nanowires due to mechanical straining [3]. The flow of charge carriers thus created will be driven to the external circuitry. Physical anisotropic properties of zincoxide are used to generate piezopotential by use of strain or by temperature. We substantiate here the conversion of heat into electric energy application through zincoxide nanowire arrays properties [4]. Amongst the zincoxide properties, together the association of the semiconducting and pyroelectric ones, engender a polarization electric field. Electric charge segregation throughout the lenght of the zincoxide nanorod is caused by the time-conditioned temperature modification. The nanogenerator we built and tested returned good values in terms of stability, having the defining factor of heat flow transformation to electric energy aprox.$0.03-0.08 Vm^2/W$. Our results exhibit the huge capability of nanowires features, piezopotential, pyroelectricity, all used in order to power nanodevices, space science, X-ray, etc. .

2. Nanogenerator architecture

Our solution of the nanogenerator pyroelectric consist in usage of the anisotropic polarization within the grown zincoxide nanowire. As consequence,

[1] Eng., University POLITEHNICA of Bucharest, Faculty of Electronics, Telecommunications and Information Technology, Bucharest, Romania, e-mail: aureliancostea@yahoo.com
[2] Prof., Optoelectronics Research Center, University POLITEHNICA of Bucharest, Romania

time-conditioned temperature fluctuation will drive electric carriers to flow [5]. The matrice of nanorods grew up on top of a Indium Tin Oxide [6] substrate. We used a growing up technique for zincoxide that relies on a watery solution. Depicted, the diameter of 200nm and the length of 2μm of the nanorods. Shown in schema, the system architecture used Fig.1c. In the contact area between the top of the zincoxide nanorods and the Ag film electrode, a Schottky contact [7] appears. At the edges of the zincoxide nanorods, a bottom electrode ITO and a top Ag film electrode are used. Both to connect the zincoxide nanodevice directly to external circuitry. The current voltage diagram points out that the nanodevice manifest a Schottky [8] characteristic at the intersection between top electrode and nanorods. We have to make sure that the charge carriers encounter no problem exiting from the nanogenerator. Thus, both the forward and reversal connections were taken under consideration in the current/ voltage output characterization.

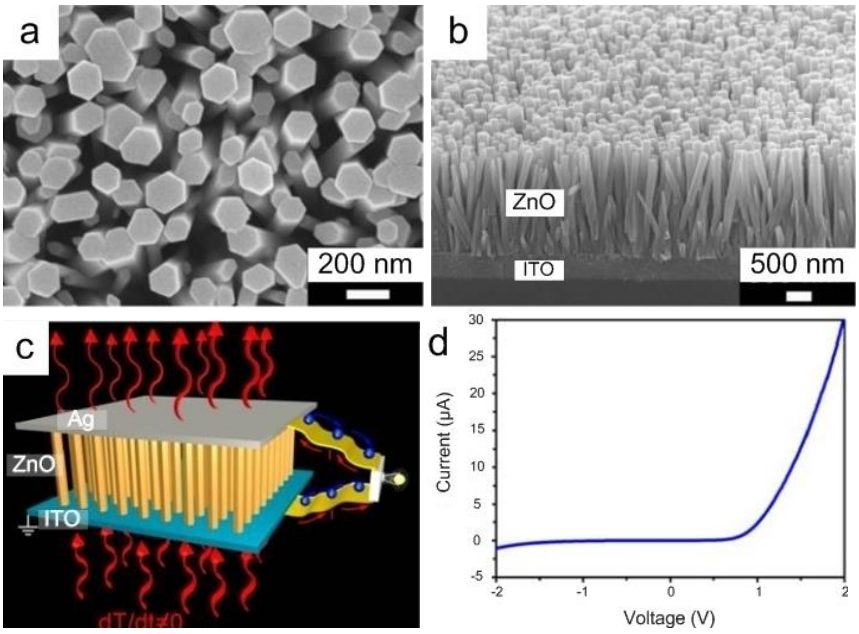

Fig. 1. (a) Array nanowire ZnO SEM picture. (b) Array nanowire ZnO SEM picture cross-sectional tilted. (c) Nanogenerator architecture. (d) current voltage nanogenerator specific features measured at temperature initially established value.

By modifying the test environment temperature in the proximity of the pyroelectric nanogenerator, we measured the nanodevice short-circuit current, also the nanodevice open-circuit voltage. Starting temperature was set up at 295K. We first modify the temperature to 289K. Then modify it back to initially 295K, then change it to 304K. Using direct connection, a negative voltage/current pointed pulse of 5.7mV/108.3pA was noticed, when a rapid decrease in temperature was applied Fig. 2a. Accordingly, a positive voltage/current pulse

was remerked when a backward rapid increase in temperature was applied, back to 295K. We connect the nanogenerator also in reverse mode and noticed that only the sign of the acquired signals was switched Fig..2c. That proves the signals we measured have been generated by the built device. Now fast increasing the temperature from initial value to 304K Fig..2d, exhibit a positive voltage/current pulse of 5.6mV/120.2pA Fig. 2e. Furthermore, a reverse connection of the nanodevice to the measurement system returned a inverted output signal Fig. 2f.

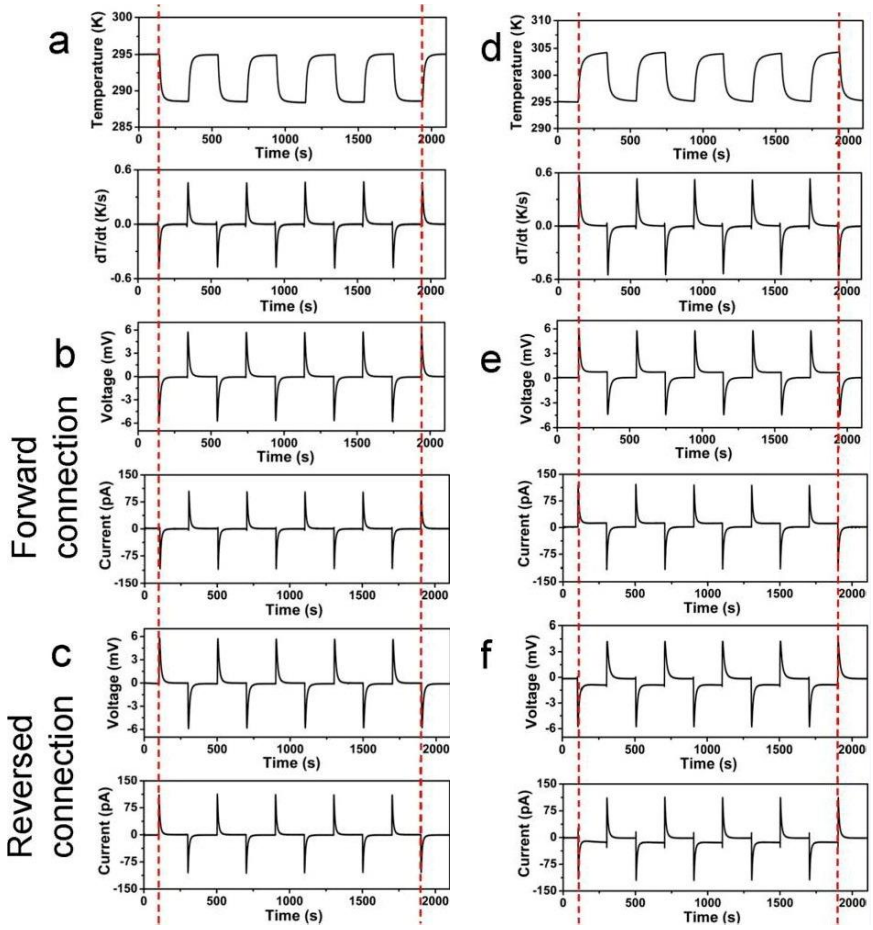

Fig. 2. (a,d) Differential curve corresponding of the nanogenerator within the cyclic changes in temperature. (b,c,e,f) The measurement system of the nanogenerator pyroelectric having forward connection and reversed connection current short-circuit and voltage open-circuit measured when aplied frequent temperature modification from (b,c) initially set up value 295K to 289K (e,f) initially set up value 295K to 304K.

If the temperature differences are getting bigger in the device, the current/voltage output peaks increase correspondingly, as shown in Fig. 3. Different magnitudes of temperature fluctuations generate correspondingly different output signals in the current/voltage diagram. Moreover, modifying the

temperature to a new lower value come up with a new peak negative value in current/voltage. The new peak negative goes back to zero when the difference in temperature disappear, Fig..3b. Rising back the temperature to the initially set up 295K, the effect in reverse was noticed. Now rising the temperature from the initially set up to a new higher value generates a positive peak in current/voltage. The current reached and stayed at a constant value instead of going to zero Fig..2e,f,3d. The acquired and kept constant value existed whilst the source of temperature was sustained. The "constant value" it is due to Seebeck [9][10] effect, inasmuch as a small temperature drop exists across the nanogenerator. We have to discriminate and separate the Seebeck effect contribution [11], wich it is not very difficult since Seebeck effect generates a dc output [12], whilst an ac output is generated by the pyroelectric [13] effect.

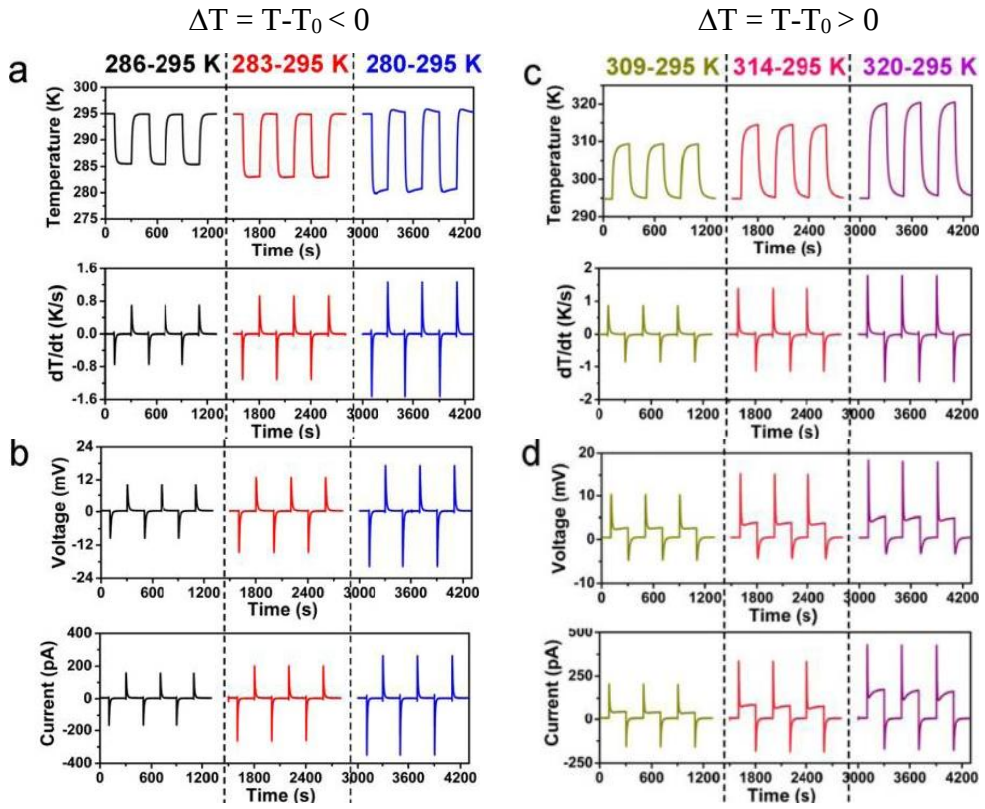

Fig. 3. (a) Decreasing of the temperature from 295 K (a) thus the output voltage and current respectively. (b) Increasing of the temperature from 295 K. (c) thus the output voltage and current respectively. (d) The noticed constant value in output voltage and current in the situation of increasing the temperature due to Seebeck effect.

The measured peaks in voltage/current are conditioned by the temperature fluctuation, substantiating almost a linear relation [14], in Fig..4a. The current pyroelectric factor and voltage pyroelectric factor are[15]:

$$P_C = \left[I/\left(A(dT/dt)\right)\right] \text{ and also } P_V = [V/(\Delta T/dt)] \quad (1)$$

notations representing as follows: r_d (aprox.32nm) - for zincoxide nanorods Debye length, ΔT - temperature fluctuations, dT/dt - temperature fluctuations ratio, A - area of the electrode, V - voltage pyroelectric, I - current pyroelectric. Throughout our experiment, we assessed pyroelectric current of aprox.1.1to1.4nC/cm^{2}K, also pyroelectric voltage of aprox.2.3−4.1×10^{4}V/mK, as represented in fig.4b. These values are superior of zincoxide material in bulk [16] 0.93nC/cm^{2}K or film [17] 1.01nC/cm^{2}K architecture. Comparing zincoxide nanorods with bulk/film-architectures [18], we remark that the zincoxide nanorods coefficients pyroelectric are enhanced. In all likelihood by having a lower density displacement, also only one crystalline structure with favourite orientations throughout the axis [19].

Transformation of the heat flow [20]

$$P_f = dF/dQ \approx V(t_0)/[Q(t_0)r_d] \quad (2)$$

has been utilised to portray the nanogenerator capacity to transform the thermal energy to the electric energy, notations representing as follows:

Q - heat energy flow per unit volume, F - pyroelectric generated electric field.

Ecuation (3)[21]

$$Q(t_0) = [(Sh)/V_0](T_0 - T_\infty) \quad (3)$$

render the Q(t_0) value, notations representing as follows: S - area surface, V0 - volume sample, h - thermal transference factor.

The thermal energy to the electric energy transformation factor P_f is aprox.0.04to0.07Vm^2/W, Fig..4c. By contrast, GaN film has aprox.2.2×10^{-3}Vm^2/W[22], lower by a factor of ten. Modifying the temperature throughout a rigorous proccess composed of 200 repetitive cycles throughout a 6 hours' time interval, Fig..4d, stability of the nanogenerator was established. During tests, no propensity of voltage signal output diminution was noted, the signal output being stable. By means of the primary pyroelectric factor, if the material dimensions are fixed, if the material volume is constant, ie can characterize the charges that are generated due to a temperature fluctuation. Fluctuations in temperature can aler the material's dimensions/volume. Deformation induced strain will occur within the anisotropic material, having as result extra contribution [23] of charges generated piezoelectrically. Mostly referred to as a pyroelectric secondary effect, has more influence and importance regarding zincoxide, cadmiumsulfide. We calculated, referring to a single zincoxide nanowire, the distributed electric potential caused by the temperature fluctuations, as shown in Fig..5. At first, to simplify the calculation, the zincoxide nanorod doping has been "ignored", "treated" as an insulator, having the diameter of 200nm and length of 2μm.

Modifying the temperature from the initially set up value to 289K, the electrical potential distribution have as result the 2.1Vto−1.7Vinterval,Fig..5a, obtained throughout orientation [0001].

By increasing the temperature from the initially set up value to 304K, we noticed an distribution in electrical potential inside −3.1V to 2.6V interval, Fig..5d. Our calculus gave us the electrical potential as being up to 3V. In relation to semiconducting zincoxide nanorods, the real electrical potential is lower than that, the measured peaks of voltage output are lower, having as reason the effect of screening [24] regarding the free charge carriers, Fig. 2,3.

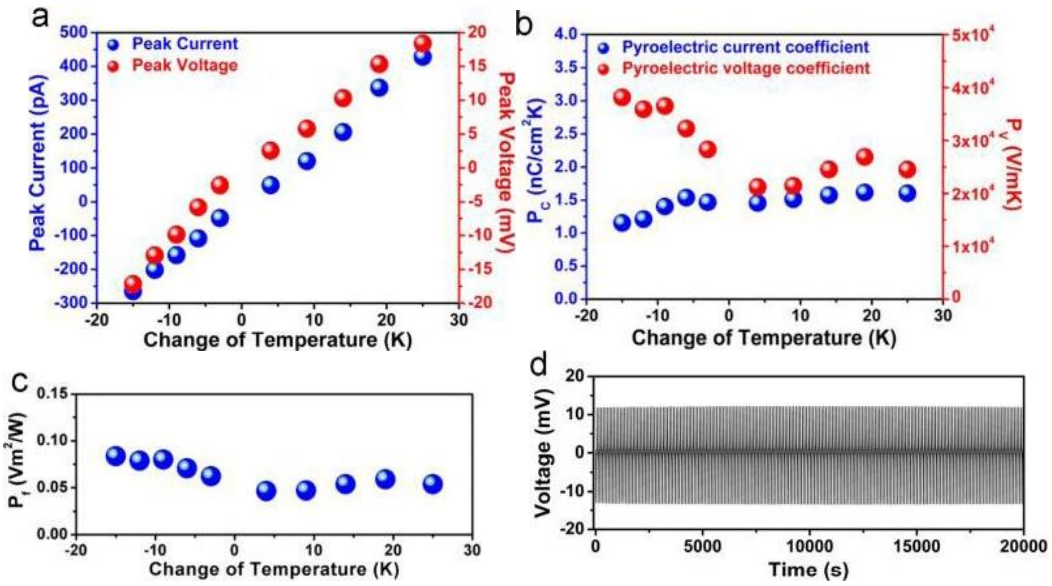

Fig. 4. The voltage/current output peak (a), coefficients voltage/current pyroelectric (b), and value characteristic within energy conversion (c), as a function of variation in temperature. (d) 200 repetitive cycles of the nanogenerator output test for stability throughout temperature fluctuation.

Within each of the contact areas, having Ag as the positive electrode and Indium tin oxide as the negative electrode, Fig..1d depicted, the barriers [25] emerge. We considered the Ag/ZnO/ITO architecture of the built device to be close to a zincoxide “sandwiched” layer. At the top and bottom, in the contact areas, device has two barrier type architectures, positioned back-to-back. Throughout a positive bias in effect, the reversed barrier between ITO and zincoxide is dominant for ITO/ZnO/Ag architecture, all the electrons flowing through ITO/ZnO/Ag. The barrier height level between the zincoxide and ITO is inferior to the zincoxide and Ag barrier hight level, depicted in Fig.5, substantiated by the inferior current values throughout negative biases, also by superior current values throughout positive biases.

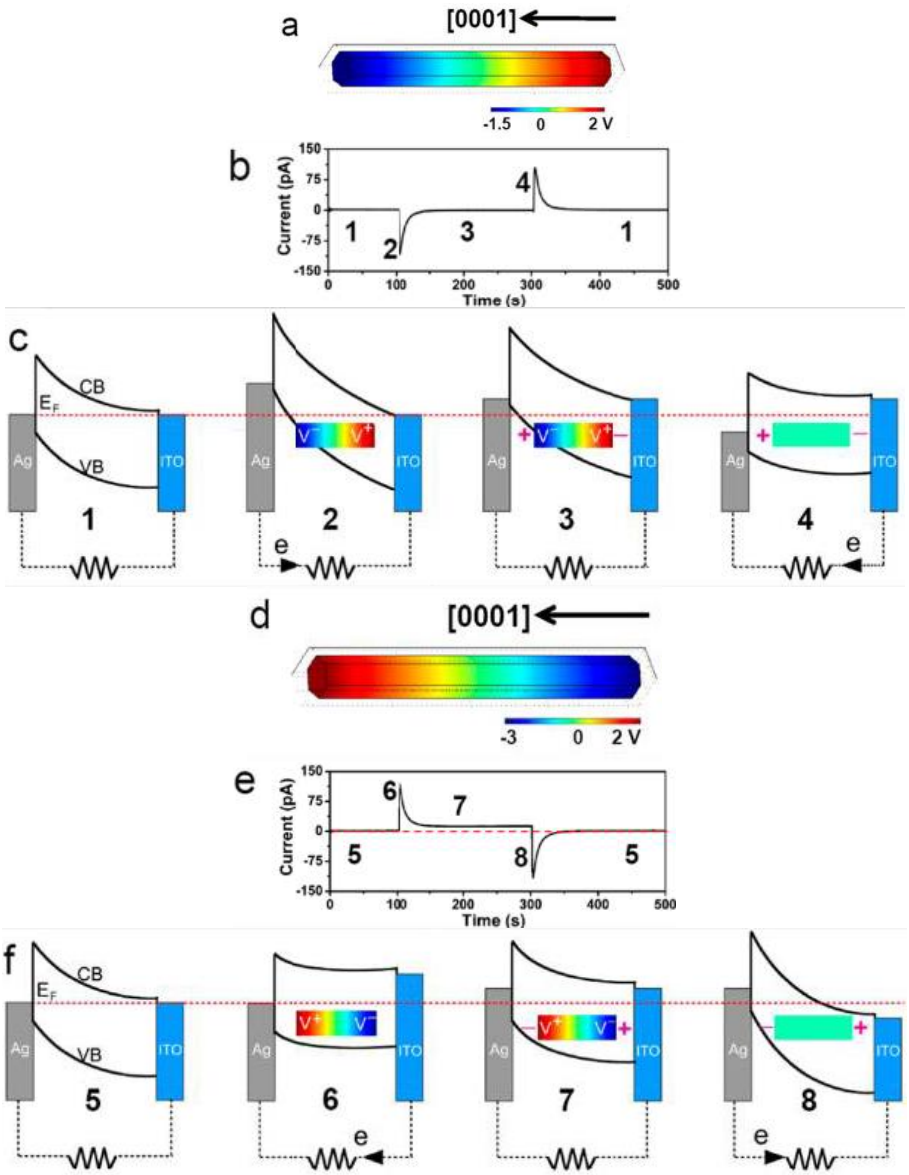

Fig. 5. (a) Having the temperature lowered from RT 295 to RT 289 K, the distribution in a single ZnO nanowire regarding the electrical potential calculated. (b,c) Having the four different stages, nominated as ("1−4"), the device diagrams of band of energy that are correspondingly with the output current measured within the experiment. (d) Having the temperature rised up from RT 295 to RT 304 K, along the [0001] direction of a single nanowire of ZnO, the distribution of the potential electric calculation. (e,f) Having the four different stages, nominated as ("5−8"), the nanogenerator diagrams of the band of energy correspondingly with the output current measured within the experiment.

Fig. 5c,f shows the functional model mechanisms proposed for the charge carriers generation, the current, in relation to the tested system structure band, subjected to temperature fluctuation.

We modify the temperature from initially set up value to 289K Fig..5c, also from initially set up value to 304K Fig. 5f. The areas labeled with “1−8” tags, Fig..5b, e, are correlated with the areas labeled with “1−8” tags, Fig. 5c,f.

Having the temperature suddenly decrease from initially set up value to 289K, inside the zincoxide nanorod is generated a pyroelectric negative field Fig..5a, throughout the [0001][26] orientation. The top electrode edge, Ag part, is in connection with positive potentials pyroelectric, whilst the bottom electrode edge, ITO part, is in connection with negative potentials pyroelectric. The Ag electrodes' Fermi level and the zincoxide nanorods conduction band can be upwarded locally by the electric negative potential, observation in concordance with the remarked negative current“2”Fig..5b. Depicted in“3”Fig..5c, no current output will be remarked if the situation of a new equilibrium value status was reached. Also, the pyroelectric potential disappears in the situation of the temperature being set back to initially set up value. The free charges carries that were accumulated at the bottom ITO negative electrode, will stream back to the top Ag positive electrode“4”Fig..5c. Rising the temperature from the initially set up value to 304K, the electric potential will begin to be positive at the top electrode and negative at the bottom ITO electrode, correspondinglyFig..5d. Having as reason the negative potential electric, the bottom ITO electrodes' Fermi level also the conduction band are lifted. That drives the charge carriers, the electrons, to move from the bottom electrode to the top electrode “6” Fig. 5f. A new value of equilibrium is reached, whereupon there should be no remarked current output. The remarked "constant value" in current “7” Fig..5f, in all likelihood it is caused by the Seebeck [27] effect and not by the pyroelectric one. Once the temperature is restored to the initially set up value of 295K, as consequence of the electrical potential fade-away [28], the accumulated charge carriers, the electrons, at the top electrode are gradually released. As result, they flow back to the bottom electrode “8” Fig..5f.

3. Conclusions and contributions.

From the start we devise of a simple single “active layer” of zincoxide nanorods acting as the “core” of the nanogenerator using the scientific data and resources available to us. Then create a procedure in order to build, test and characterize the zincoxide nanorods architecture for thermoelectric energy harvesting.

Throughout the entire experiment we contributed successfully, step by step, to conceive, build and test our solution architecture. We approached the

pyroelectric nanogenerator as a basic “sandwiched layer” of zincoxide nanorods architecture for thermoelectric energy harvesting. For the zincoxide nanorods we used, mean value for diameter is +/-200nm, the pyroelectric voltage factor is $2.3{-}4.1\times10^{4}$V/mK, also the pyroelectric current factor is $1.1{-}1.4$nC/cm^{2}K.

We approached a simple new architecture of nanogenerator. That constitute a contribution to further develop the base for nanotechnologyies that aspire to be self-powered. Here, improving thermal energy harvesting relying on the highly time-constrained temperature fluctuation is the key factor. Used in practical solutions such as sensors in wireless networks, imaging through temperature, diagnostics in medical sciences, microelectronics for personal usage.

Regarding building method contribution, first of all, from ”bottom” to ”top”, layer by layer, nanodevice architecture building steps are: a ”first” layer of a thin glass substrate, a 500nm ”second” ITO layer and a ”third”, on top, 50nm zincoxide seed layer. Performing the growth of the nanowire was achieved by a hydrothermal method, relying on the zincoxide seed layer. In order to successfully grown the arrays of zincoxide nanowire, we utilize an solution composed of Zn-$(NO_3)_2\cdot6H_2O$ and hexamethylenetetramine, each in equal concentrations of 50mM. The oven we used had mechanical convection capability at 85°C for the time of10hours, where everything took place. At the surface, on the solution, the substrate stood afloat with one face down (indium tin oxide), due to the surface tension.

On top of the nanogenerators’ zincoxide nanowire arrays, we lay down a silver film. The silver film serves also as the top electrode. Nanogenerators’ area is aprox.14mm^2. Temperature modification of the nanogenerator was realized by using a thermoelectric controlled cooler and heater. Throughout the experiments, we acquire and record all the temperatures of the zincoxide nanorod arrays, by means of temperature sensors previously installed. For all the time of the experiments, we did not apply any external power to the nanogenerators’ circuit. All the measurements were realised only with a low-noise voltage/current preamplifier.

Acknowledgments

The activities presented in this paper were performed in the frame of two programs: Project PN - III - P1-1.2-PCCDI-2017-0560, “Eco-nano-technologies and smart equipment for mapping the soil parameters and plant growth dynamics in order to increase the efficiency of agricultural production and environmental protection - ENI”, under contract no. 41PCCDI/2018, and respectively Project PN-III-P1-1.2-PCCDI-2017-0419, “Sensors and electronic and photonic integrated systems for the security of people and infrastructures - SENSIS”, under contract no. 71PCCDI 2018.

REFERENCES

[1]. Lawrence Livermore National Laboratory, "Estimated energy use in 2010: 98 quads". https://flowcharts.llnl.gov/, (accessed 2010).
[2]. DiSalvo, F. J. Science 1999, 285, 703−706.
[3]. Bell, L. E. Science 2008, 321, 1457−1461.
[4]. Lang, S. B. Sourcebook of pyroelectricity; Gordon & Breach Science: London, 1974.
[5]. Morozovska, A. N.; Eliseev, E. A.; Svechnikov, G. S.; Kalinin, S. V. J. Appl. Phys. 2010, 108, 042009.
[6]. Wang, Z. L.; Song, J. H. Science 2006, 14, 242−246.
[7]. Wang, X. D.; Song, J. H.; Liu, J.; Wang, Z. L. Science 2007, 316, 102−105.
[8]. Qin, Y.; Wang, X. D.; Wang, Z. L. Nature 2008, 451, 809−813.
[9]. Yang, R. S.; Qin, Y.; Dai, L. M.; Wang, Z. L. Nat. Nanotechnol. 2009, 4, 34−39.
[10]. Lang, S. B. Phys. Today 2005, 58, 31−36.
[11]. Cooper, J. Nature 1962, 194, 269−271.
[12]. Brownridge, J. D. Nature 1992, 358, 287−288.
[13]. Hu, Y. F.; Zhang, Y.; Xu, C.; Lin, L.; Snyder, R. L.; Wang, Z. L., Nano Lett. 2011, 11, 2572−2577.
[13]. Lang, S. B.; Tofail, S. A. M.; Gandhi, A. A.; Gregor, M.; Wolf-Brandstetter, C.; Kost, J.; Bauer, S.; Krause, M. Appl. Phys. Lett. 2011, 98, 123703.
[14]. Bykhovski, A. D.; Kaminski, V. V.; Shur, M. S.; Chen, Q. C.; Khan, M. A. Appl. Phys. Lett. 1996, 69, 3254−3256.
[15]. Ye, C.; Tamagawa, T.; Polla, D. L. J. Appl. Phys. 1991, 70, 5538−5543.
[16]. Zook, J. D.; Liu, S. T. J. Appl. Phys. 1978, 49, 4604−4606.
[17]. Gao, Y.; Wang, Z. L. Nano Lett. 2009, 9, 1103−1110.
[18]. Yang, Y.; Guo, W.; Zhang, Y.; Ding, Y.; Wang, X.; Wang, Z. L., Nano Lett. 2011, 11, 4812−4817.
[19]. Katz, E.; Bückmann, A. F.; Willner, I. Self-Powered Enzyme-Based Biosensors. J. Am. Chem. Soc. 2001, 123, 10752–10753.
[20]. Dondi, D.; Bertacchini, A.; Larcher, L.; Brunelli, D.; Benini, L. Modeling and Optimization of a Solar Energy Harvester System for Self-Powered Wireless Sensor Networks. IEEE Trans. Ind. Electron. 2008, 55, 2759–2766.
[21]. Hu, Y.; Zhang, Y.; Xu, C.; Lin, L.; Snyder, R. L.; Wang, Z. L. Self-Powered System with Wireless Data Transmission. Nano Lett. 2011, 11, 2572–2577.
[22]. Xu, S.; Qin, Y.; Xu, C.; Wei, Y.; Yang, R.; Wang, Z. L. Self-Powered Nanowire Devices. Nat. Nanotechnol. 2010, 5, 366–373.
[23]. Wang, Z. L.; Song, J. H. Piezoelectric Nanogenerators Based on Zinc Oxide Nanowire Arrays. Science 2006, 312, 242–246.
[24]. Qin, Y.; Wang, X. D.; Wang, Z. L. MicrofibreNanowire Hybrid Structure for Energy Scavenging. Nature 2008, 451, 809–813.
[25]. Hu, Y.; Lin, L.; Zhang, Y.; Wang, Z. L. Replacing a Battery by a Nanogenerator with 20 V Output. Adv. Mater. 2012, 24, 110–114.
[26]. Tian, B.; Zheng, X.; Kempa, T. J.; Fang, Y.; Yu, N.; Yu, G.; Huang, J.; Lieber, C. M. Coaxial Silicon Nanowires as Solar Cells and Nanoelectronic Power Sources. Nature 2007,449, 885–890.
[27]. Yang, Y.; Guo, W.; Zhang, Y.; Ding, Y.; Wang, X.; Wang, Z. L. Piezotronic Effect on the Output Voltage of P3HT/ZnO Micro/Nanowire Heterojunction Solar Cells. Nano Lett.2011, 11, 4812–4817.
[28]. Yan, X.; Poudel, B.; Ma, Y.; Liu, W. S.; Joshi, G.; Wang, H.; Lan, Y. C.; Wang, D. Z.; Chen, G.; Ren, Z. F. Experimental Studies on Anisotropic Thermoelectric Properties and Structures of n-Type $Bi_2Te_{2.7}Se_{0.3}$. Nano Lett. 2010, 10, 3373–3378.